Fig. 2. Comparison of island arc tonalite compositions from Fiji, Guadalcanal, western North America, and Newfoundland (filled circles) (*2, 3, 5, 14, 16*) with experimental results. There is excellent agreement between closed system experimental melt compositions and the natural data, little agreement between the 1-kbar water-saturated results and the natural data, and virtually no overlap between the 3-kbar water-saturated experimental melts and the natural tonalites. All compositions normalized to 100%, volatile-free; n = number of experiments.

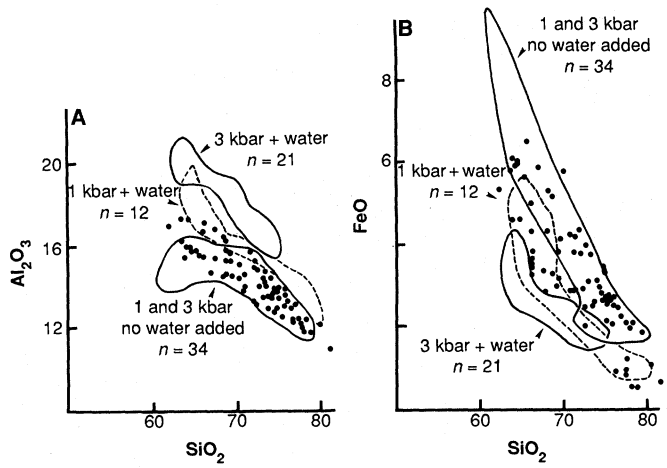

crustal pressures in a closed system. A likely place for such melting to occur is at or near the contact between hydrated arc crust and a hot basaltic intrusion. Local zones of melting have been observed around basaltic intrusions and elsewhere in several ancient island arc basement complexes (*6, 14*). Significant volumes of silicic magma can be generated by basalt-induced melting even of relatively mafic island arc crust (*15*), potentially enough to account for the observed abundance of island arc tonalite. Our experiments predict that dehydration melting will leave an anhydrous "granulitic" restite; rocks having the proper restite mineralogy have been described from at least one contact aureole (*6*). At water pressures as low as 1 kbar, there is significant divergence of experimental melt compositions and the natural data set, and by 3-kbar water pressure, the compositions are distinctly different. Indications from this and other studies are that the compositional gap between natural and experimentally produced melts increases as water pressure increases. Thus water-saturated melting of arc crust at pressures greater than 1 kbar is an unlikely mechanism for the formation of island arc tonalite.

REFERENCES AND NOTES

1. F. Barker, in *Trondhjemites, Dacites and Related Rocks*, F. Barker, Ed. (Elsevier, New York, 1979), pp. 1–12; A. R. Chivas, A. S. Andrews, A. K. Sinha, J. R. O'Neil, *Nature* **300**, 139 (1982); J. B. Whalen, *J. Petrol.* **26**, 603 (1985); J. S. Beard, H. W. Day, *Geol. Soc. Am. Bull.* **99**, 779 (1987).
2. J. B. Gill and A. L. Stork, in *Trondhjemites, Dacites and Related Rocks*, F. Barker, Ed. (Elsevier, New York, 1979), pp. 629–649.
3. D. Phelps, in *ibid*, p. 547–580.
4. F. Barker and J. G. Arth, *Geology* **4**, 596 (1976); W. P. Leeman and D. R. Smith, *Goldschmidt Conference Program and Abstracts* (The Geochemical Society, State College, PA, 1988), p. 57; R. P. Rapp, B. E. Watson, C. F. Miller, *ibid*, p. 69; M. J. Rutter and P. J. Wyllie, *Nature* **331**, 159 (1988).
5. J. G. Payne and D. F. Strong, in *Trondhjemites, Dacites and Related Rocks*, F. Barker, Ed. (Elsevier, New York, 1979), pp. 489–516.
6. J. S. Beard, *Geol. Soc. Am. Abstr. Prog.* **19**, 357 (1987).
7. J. R. Holloway, in *Research Techniques for High Pressure and High Temperature*, G. C. Ulmer, Ed. (Springer-Verlag, New York, 1971), pp. 217–258. G. E. Lofgren, in *Hydrothermal Experimental Techniques*, G. C. Ulmer and H. L. Barnes, Eds. (Wiley-Interscience, New York, 1987), pp. 329–332.
8. With increasing temperature, the Si and K contents of melts decreased and the Fe, Mg, and Ca contents increased.
9. M. C. Gilbert, R. T. Helz, R. K. Popp, F. S. Spear, in *Amphiboles: Petrology and Experimental Phase Relations*, vol. 9B of *Reviews in Mineralogy*, D. R. Veblen and P. H. Ribbe, Eds. (Mineralogical Society of America, Washington, DC, 1982), pp. 229–354.
10. C. W. Burnham, in *The Evolution of Igneous Rocks, Fiftieth Anniversary Perspectives*, H. S. Yoder, Ed. (Princeton Univ. Press, Princeton, NJ, 1979), pp. 439–482; J. A. Whitney, *J. Geol.* **83**, 1 (1975); M. T. Naney and S. E. Swanson, *Am. Mineral.* **65**, 639 (1980); D. R. Baker and D. H. Eggler, *ibid* **72**, 12 (1987).
11. R. T. Helz, *J. Petrol.* **14**, 249 (1973); *ibid* **17**, 139 (1976).
12. S. D. Spulber and M. J. Rutherford, *ibid.* **24**, 1 (1983).
13. P. J. Wyllie, *Tectonophysics* **43**, 41 (1977).
14. J. Malpas, in *Trondhjemites, Dacites and Related Rocks*, F. Barker, Ed. (Elsevier, New York, 1979), pp. 465–488.
15. H. E. Huppert and R. S. J. Sparks, *J. Petrol.* **29**, 599 (1988).
16. A. R. Chivas, *thesis*, University of Sydney (1977); F. Barker, H. T. Millard, Jr., R. J. Knight, in *Trondjemites, Dacites and Related Rocks*, F. Barker, Ed. (Elsevier, New York, 1979), pp. 531–546; J. S. Beard, unpublished data.
17. We thank A. Lanier and W. Carter for their help with the high-pressure–high-temperature equipment and G. McKay and V. Yang for access to and help in using the microprobe facility at Johnson Space Center (JSC). Early versions of this manuscript were reviewed by D. Elthon, J. Jones, and P. Thy. This work was done while the senior author held a National Research Council Fellowship at JSC.

27 December 1988; accepted 23 February 1989

Contribution of Ultraviolet Irradiance Variations to Changes in the Sun's Total Irradiance

J. LEAN

The sun's total irradiance decreased from 1980 to mid-1985, remained approximately constant until mid-1987, and has recently begun to increase. This time interval covered the decrease in solar activity from the maximum of solar cycle 21 to solar minimum and the onset of cycle 22. The sun's ultraviolet irradiance also decreased during the descending phase of cycle 21 and, like the total irradiance, is now increasing concurrently with the increase in cycle 22 activity. Although only 1 percent of the sun's energy is emitted at ultraviolet wavelengths between 200 and 300 nanometers, the decrease in this radiation from 1 July 1981 to 30 June 1985 accounted for 19 percent of the decrease in the total irradiance over the same period.

DURING THE RECENT SUNSPOT CYCLE 21, changes in the sun's total irradiance and in its emission at ultraviolet (UV) wavelengths were observed simultaneously from space by a variety of independent experiments. Understanding the nature and origin of this variability is important because solar irradiance variations over longer time scales have been invoked as drivers of tropospheric change, for example, in the sea-surface temperature (*1*) and in climate (*2*), including the Maunder Minimum climate anomaly. Although the spectrum of the radiation that composes the sun's total irradiance is well known, the contribution of irradiance variations in specific spectral bands to changes in the total irradiance is less certain (*3*). These irradiance variations are of interest for solar studies as a tool for probing the physical origins of the variability. They are also of interest for climate studies because variations in the total solar irradiance measured from a satellite platform must be separated into changes in that part of the solar spectrum incident on the earth's surface and changes in the solar UV spectrum at wavelengths less than 300 nm that is absorbed in the earth's atmosphere. The UV energy emitted by the sun is known to be more variable than its visible radiation. This difference in variability suggests that, although only ~1% of the sun's

E. O. Hulburt Center for Space Research, Naval Research Laboratory, Washington, DC 20375.

electromagnetic energy is radiated at wavelengths shorter than 300 nm, changes in this radiation may account for significantly more than 1% of the variations in the sun's total irradiance.

Both the UV irradiances and the total irradiance vary throughout the 11-year sunspot cycle, reaching their peak values at times near the maximum of solar activity. Measurements by the Earth Radiation Budget (ERB) radiometer on the Nimbus 7 satellite and the Active Cavity Radiometer (ACRIM) on the Solar Maximum Mission (SMM) have shown that during solar cycle 21 the peak-to-peak amplitude of the 11-year variation in the sun's total irradiance was approximately 0.08% (*4, 5*). Solar observations at UV wavelengths, made during solar cycle 21 by the Solar Backscatter Ultraviolet (SBUV) experiment on the Nimbus 7 satellite, and by the solar spectrometer on the Solar Mesosphere Explorer (SME) have established that the magnitude of the sun's UV irradiance variations over the 11-year cycle is approximately a factor of 2 at Lyman α (121.6 nm), decreasing to 10% at 200 nm, 5% at 250 nm, and less than 1% at wavelengths longer than 300 nm (*6*). These UV irradiance variations are thus considerably larger than the 0.08% solar cycle variation in the total irradiance.

Quantitative evaluation of the contribution of UV irradiance variations to changes in the sun's total irradiance has been hindered by a lack of accurate UV irradiance measurements at different phases of the 11-year solar cycle (*7–9*). Concurrent ACRIM, ERB, SME, and SBUV data now make it possible to investigate this question. Shown in Fig. 1 are the sun's total irradiance and UV irradiances at Lyman α and the wavelength intervals 200 to 250 nm and 250 to 300 nm during most of solar cycle 21. The data in Fig. 1 are 81-day running means of the daily observations, so that day-to-day fluctuations associated with the 27-day solar rotation are not shown but intermediate and long-term trends are emphasized. Note that 3 W m^{-2} has been subtracted from the ERB data, to account for the difference in absolute calibration between the ACRIM and ERB radiometers. Solar UV irradiance data at wavelengths longer than 200 nm have been normalized to measurements made in August 1985 by the Solar Ultraviolet Spectral Irradiance Monitor (SUSIM) flown on Spacelab-2 (*10*). With a reported uncertainty of better than 5%, the SUSIM UV irradiance measurements are the most accurate now available.

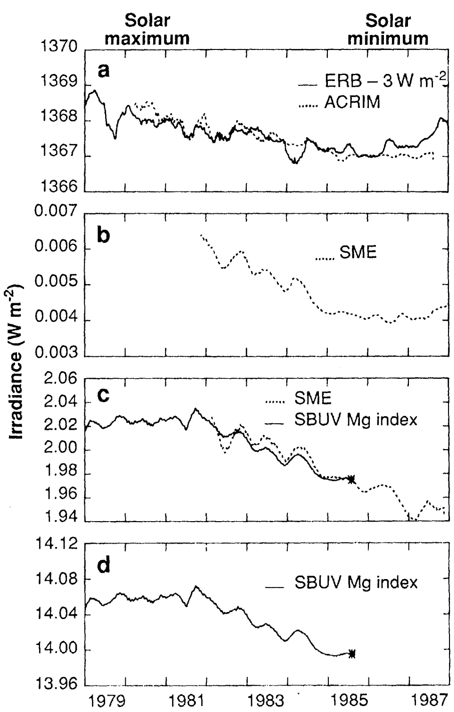

Fig. 1. Variations in the sun's emission during the declining phase of solar cycle 21, as evidenced by 81-day running means of (**a**) the total irradiance (*4, 5*) and the UV irradiance at (**b**) Lyman α and in the wavelength intervals (**c**) 200 to 250 nm and (**d**) 250 to 300 nm (*6, 13*). The asterisks are the SUSIM measurements (*10*).

Long-term, downward trends, coincident with the decrease from maximum to minimum solar activity, are evident in Fig. 1 in both the ACRIM and ERB total irradiance data and in the SME and SBUV spectral UV irradiance data. Similarities and differences between the ACRIM and ERB measurements before 1985 have been discussed elsewhere (*9*). Their somewhat different upward trends since then are still being investigated. At the UV wavelengths, solar irradiance measurements made by SME are potentially more reliable than those made directly by SBUV for determining long-term trends. This is so because the SME instrument carried stored, reference diffusers that have allowed an assessment of long-term changes in its responsivity associated with changes in diffuser reflectivity. However, the stated long-term precision of the SME solar irradiance data base is $\pm 2\%$ per year, a value that exceeds the observed changes at wavelengths longer than 250 nm. Ongoing analysis of the SME instrument performance, especially relative to small temperature effects in the wavelength drive system, may soon improve the long-term precision of the SME irradiance measurements (*11*). The SBUV experiment, despite significant degradation in its diffuser reflectivity, has provided precise observations of long-term changes in the emission from the core of the Mg II Fraunhofer doublet near 280 nm, relative to emission in the wings of the doublet (*12*). Ratios of the core emission to the wing emission, known as the Mg index, have been used in conjunction with observations of the short-term UV irradiance variations associated with solar rotation to generate irradiance variations at UV wavelengths longer than 160 nm (*12, 13*), and it is these data that are shown in Fig. 1. The agreement between the SME and SBUV data at 200 to 250 nm gives confidence that the variations shown in Fig. 1 are indeed of solar, rather than instrumental, origin.

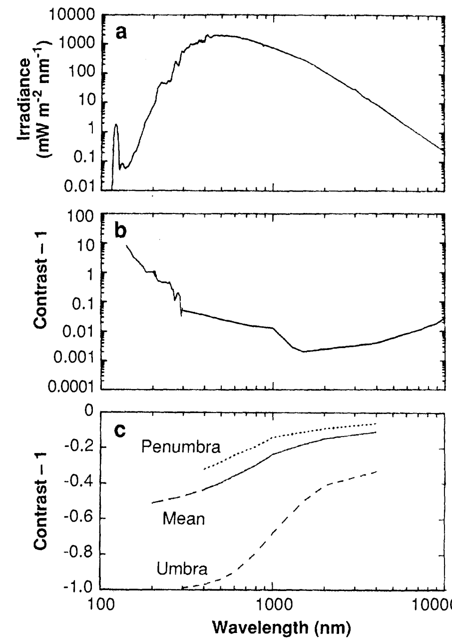

Fig. 2. Spectrum of (**a**) the sun's electromagnetic radiation, together with estimates of the contrast of (**b**) faculae and (**c**) sunspot umbrae and penumbrae (*20*).

To estimate the downward trends in the irradiance in Fig. 1, linear fits were calculated for the daily data between 1 July 1981 (when the UV irradiances were near their maximum values) and 30 June 1985 (near minimum solar activity). From regressions of the ACRIM and ERB data against day number, values for the decrease in the total solar irradiance, S, over this period were determined to be 0.78 and 0.64 W m^{-2}, respectively, with a mean value of ΔS = 0.71 W m^{-2}. UV irradiance changes obtained from regressions of the SME Lyman α data and the SBUV Mg index data against day number, over this same period, are given in Table 1. Coincident with a decrease in S of ΔS = 0.71 W m^{-2} was a decrease of 0.0025 W m^{-2} at Lyman α and 0.136 W m^{-2} at 200 to 300 nm. Variations in the Lyman α emission during this time period thus accounted for 0.35% of the change in S, even though the energy contributed to S by Lyman α radiation is negligible (<0.0004%). Changes in the solar spectrum at wavelengths between 200 and 300 nm accounted for 19% of the decrease in the total radiative output, although only

Table 1. Contribution of the solar UV spectral irradiance, I, to the total solar irradiance, S = 1366.8 W m^{-2}, and of ΔI over the period 1 July 1981 to 30 June 1985 to ΔS = 0.71 W m^{-2}. The contribution of ΔI to the change in the total irradiance corrected for sunspot blocking, ΔS_c = 1.86 W m^{-2}, is also given. Values of I are from (10), measured near minimum solar activity, and S is the solar minimum value of the total irradiance measured by ACRIM. The values of ΔS and ΔS_c used here are averages determined from the ACRIM and ERB measurements.

Wavelength (nm)	I (W m^{-2})	I as % of S	ΔI (W m^{-2})	ΔI as % of ΔS	ΔI as % of ΔS_c
121.6 (Lα)	0.004	<0.0004	0.0025	0.35	0.13
200–250	1.97	0.14	0.059	8.3	3.2
250–300	14.0	1.02	0.077	10.8	4.1
300–350*	43.11	3.15	0.031	4.4	1.7
350–400*	61.76	4.52	0.061	8.6	3.3
Sum	120.84	8.83	0.23	32.1	12.3

*See text.

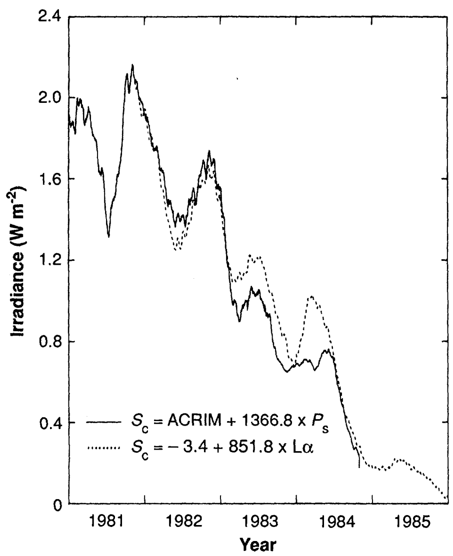

Fig. 3. Variations in S_c, the total solar irradiance corrected for the effect of sunspots by removing P_s from the ACRIM total irradiance observations (solid line), compared with the variations in the Lyman α (Lα) irradiance variations measured by SME (dotted line). For comparison with S_c, the Lyman α data have been transformed to an equivalent S_c by linear regression. The data shown are 81-day running means of the daily observations.

1.16% of S is emitted in this wavelength band.

Solar spectral irradiance variations at wavelengths longer than ~300 nm were not measured by SME, but estimates obtained from the Mg index indicate a decrease of 0.092 W m^{-2} in the solar irradiance between 300 and 400 nm. Changes in this UV radiation, which contributes 7.7% of the total irradiance, may therefore account for an additional 13% of the total irradiance variations over this time interval, with the following caveat. In estimates of long-term irradiance variability based on the Mg index it is assumed that the origins of both the long-term and the short-term variations are identical, that is, enhanced emission from bright active regions. This assumption becomes increasingly less valid for irradiance variations at wavelengths increasingly longward of 300 nm because, as discussed below, the contribution of sunspot darkening to solar irradiance variations increases with wavelength.

Although both the total and the UV irradiances exhibit overall, long-term, downward trends during the declining phase of solar cycle 21, there is not a simple linear relation between their variations throughout the entire solar cycle. This is so because variations in the total solar irradiance result from the competing effects of both bright and dark active regions, that is, faculae and sunspots (14, 15), whereas bright active regions alone are the dominant source of irradiance variability at wavelengths shorter than 250 nm (16, 17).

Sunspots are regions in the photosphere where the heat flow is inhibited, with a reduction in emission corresponding to the reduced temperature. Faculae are those magnetic regions in the sun's photosphere where the emission from the visible continuum is enhanced above that from the surrounding quiet sun (18). When the sun's disk is viewed at the shorter UV wavelengths corresponding to light emitted higher in the solar atmosphere, bright active regions, called plages, are observed approximately cospatially with the photospheric faculae. Thus the terms faculae and plages typically refer to bright active regions viewed, respectively, at visible and UV wavelengths. In general, plages cover approximately an order of magnitude more of the sun's disk and are longer lived than sunspots (19).

Figure 2 illustrates the spectrum of the sun's radiation and the spectral contrasts of both bright faculae-plages and dark sunspots (20). The contrast is the ratio of the specific radiance from an active region relative to that from the nearby, background quiet sun. When observed at UV wavelengths, sunspots are darker and plages are brighter, relative to the background quiet sun, than when they are observed in the visible region of the spectrum. But, whereas the excess emission (contrast − 1) from bright active regions increases by approximately two orders of magnitude as the wavelength decreases from 500 to 200 nm, there is a much smaller corresponding increase of only 35% in the sunspot emission deficit. This explains why, relative to faculae, sunspots play an important role in the variability of solar radiation at wavelengths between 400 and 800 nm, which composes 48% of the total irradiance, but only a minor role in the variability of radiation at wavelengths less than 300 nm. And it is because sunspots do not block the sun's UV radiation in the same way that they block its visible emission that UV irradiance variations account for such a significant fraction of the variations in the sun's total irradiance.

That the sun's total irradiance is brighter, rather than dimmer, during times of peak solar activity indicates that there is a source of enhanced emission that varies over the 11-year cycle, and whose integrated radiation more than compensates for the decreased output in the region of sunspots (9, 15). To better understand the temporal behavior of this brightness source, the bolometric sunspot blocking function, P_s, can be used to remove from the measured total irradiances those variations associated only with sunspots (9, 21). Converting P_s to watts per square meter and removing it from the ACRIM S measurements yields the corrected irradiances, $S_c = S + 1366.8 \times P_s$, shown in Fig. 3. Also shown in this figure are the SME Lyman α irradiances, which have been transformed to an equivalent S_c by linear regression. It is clear in Fig. 3 that S_c and the Lyman α irradiances behave remarkably similarly throughout the entire descending phase of the solar cycle, presumably because they are both varying in response to changes in a common source of enhanced emission on the solar disk, S_c at all wavelengths and Lyman α in only the UV portion of the spectrum. Because of sunspot blocking, the solar cycle variation in S is smaller than that in S_c so that the UV irradiance variations account for a larger fraction of the variability in S than in S_c. Over the period 1 July 1981 to 30 June 1985, the change in S_c, determined from linear regression of S_c against day number, exhibited values of 2 and 1.74 W m^{-2}, from the ACRIM and ERB measurements, respectively. Included in Table 1 are estimates of the contribution of the UV irradiance variations to ΔS_c = 1.86 W m^{-2} (the mean value of the ACRIM and ERB estimates). The decrease of 0.14 W m^{-2} at wavelengths between 200 and 300 nm accounts for 7% of ΔS_c, compared with 19% of ΔS.

Earlier investigators have shown that the variation in S_c is similar to the variation in the strengths of various Fraunhofer lines from the mid-photosphere and chromosphere and have concluded that the source of the solar cycle variation in S_c is the facular brightening associated with magnetic fields that penetrate the upper layers of the solar atmosphere (*9, 22*). The correspondence between changes in S_c and in the Lyman α radiation, which is formed in the upper chromosphere, supports this idea. Other studies, however, have suggested that only part of the physical origin of the S_c variation is facular, the remainder being attributed to either global pulsations (*5*) or photospheric temperature variations (*23*). It remains to be seen whether mechanisms for S_c variations, other than a solar cycle variation in facular emission, can also account for coupling between S_c and the Lyman α emission.

It will be of interest, in the future, to determine how changes in the entire solar spectrum, not just the UV portion, correspond to variations in total irradiance. In particular, measurements of irradiance variations at wavelengths from 300 to 400 nm, which may account for some 13% of the total irradiance variability, have yet to be made with sufficient precision to permit a reliable evaluation of the contribution of this spectral region to total irradiance variability or to establish the relative roles of sunspots and faculae for understanding either the day-to-day variations or the solar cycle trends. Simultaneous observations by ACRIM II and SUSIM, both to be launched on the Upper Atmosphere Research Satellite, should allow an improved understanding of both the total and the UV solar irradiance variations.

REFERENCES AND NOTES

1. G. Reid, *Nature* **329**, 142 (1987).
2. J. Hanson *et al.*, *J. Geophys. Res.* **93**, 9341 (1988).
3. O. R. White, Ed., *The Solar Output and Its Variations* (Colorado Associated Univ. Press, Boulder, 1977).
4. The ERB and ACRIM radiometers on the Nimbus 7 and SMM satellites, respectively, are discussed by J. R. Hickey *et al.* [*Science* **208**, 281 (1980)] and by R. Willson [*Appl. Opt.* **18**, 179 (1979)]. Recent results from the ERB and ACRIM experiments are described by J. R. Hickey *et al.* [in *Solar Radiative Output Variations*, P. Foukal, Ed. (Cambridge Research and Instrumentation, Inc., Cambridge, MA, 1987), p. 189] and in (*5*).
5. R. C. Willson and H. S. Hudson, *Nature* **332**, 810 (1988).
6. Estimates of solar cycle UV irradiance variations from SBUV observations have been reported by D. F. Heath and B. M. Schlesinger [in *IRS 84: Current Problems in Atmospheric Radiation, Proceedings of the International Radiation Symposium*, G. Fiocco, Ed. (Deepak, Hampton, VA, 1984), p. 315. Long-term trends measured by the SME have been described by G. Rottman [in *Solar Radiative Output Variations*, P. Foukal, Ed. (Cambridge Research and Instrumentation, Inc., Cambridge, MA, 1987), p. 71; *Adv. Space Res.* **8** (no 7), 53 (1988). Solar UV irradiance variations have been reviewed by J. Lean [*J. Geophys. Res.* **92**, 839 (1987)].
7. J. Lean *et al.*, in *Solar Irradiance Variations on Active Region Time Scales*, B. LaBonte, H. Hudson, G. Chapman, Eds. (NASA Conference Publication 2310, National Aeronautics and Space Administration, Washington, DC, 1984), p. 253.
8. J. Lean, *J. Geophys. Res.* **89**, 1 (1984).
9. P. Foukal and J. Lean, *Astrophys. J.* **328**, 347 (1988).
10. M. E. VanHoosier *et al.*, *Astrophys. Lett. Commun.* **27**, 163 (1988). The SUSIM Spacelab-2 solar irradiance measurements at wavelengths longer than 200 nm agree to within a few percent with the measurements from Spacelab-1 by D. Labs *et al.*, *Sol. Phys.* **107**, 203 (1987).
11. Because of recently identified temperature-dependent wavelength calibration drifts in the SME solar spectrometer measurements throughout the measurement period, the data shown in Fig. 1, which are those currently available from the SME on-line data base, are being revised (G. Rottman, private communication).
12. B. M. Schlesinger and D. F. Heath, *J. Geophys. Res.* **93**, 7091 (1988).
13. D. F. Heath and B. M. Schlesinger, *ibid.* **91**, 8672 (1986).
14. P. Foukal and J. Lean, *Astrophys. J.* **302**, 826 (1986).
15. The roles of sunspot and facular emissions in total irradiance variations on solar cycle time scales have been discussed by J. Lean and P. Foukal [*Science* **240**, 906 (1988)], K. Schatten [*Geophys. Res. Lett.* **15**, 121 (1988)], and Willson and Hudson (*5*).
16. The correspondence between solar UV irradiance variations and changes in solar Ca II K plage emission has been reported at wavelengths from 140 to 210 nm by Cook *et al.* (*17*) and J. L. Lean *et al.* [*J. Geophys. Res.* **87**, 10307 (1982)], and at wavelengths from 200 to 300 nm by Lean (*8*).
17. J. W. Cook *et al.*, *J. Geophys. Res.* **85**, 2257 (1980).
18. F. Q. Orrall, Ed., *Solar Active Regions* (Colorado Associated Univ. Press, Boulder, 1981).
19. C. W. Allen, *Astrophysical Quantities* (Athlone, London, 1973), p. 188.
20. The solar spectrum data are from (*10*) for wavelengths shorter than 400 nm and from (*3*) at longer wavelengths. The facular contrasts at wavelengths from 140 to 200 nm are from measurements reported by Cook *et al.* (*17*). At wavelengths from 200 to 300 nm the contrasts were derived from model calculations based on the World Data Center Ca II K plage areas and the SBUV irradiance measurements as described by Lean (*8*). Contrast estimates at wavelengths longer than 300 nm are from the facular model of M. Herse [*Sol. Phys.* **63**, 35 (1979)], normalized to ~2% at 530 nm, following P. Foukal, in *The Physics of Sunspots*, L. E. Cram and J. H. Thomas, Eds. (Sacramento Peak Observatory, Sunspot, NM, 1981), p. 391. Facular contrasts are poorly known and highly model-dependent. The data shown in Fig. 2 are intended to show, in a qualitative way only, the wavelength dependence of the facular contrast. The sunspot contrasts are from (*19*), p. 184. More recent measurements by F. Albregtsen and P. Maltby [*Sol. Phys.* **71**, 269 (1981)] confirm the general trend of sunspot contrast with wavelength.
21. The sunspot blocking function, P_s, is an estimate of the fraction of the sun's irradiance that is blocked by sunspots. It is available from the World Data Center of the National Oceanic and Atmospheric Administration. Its calculation is described in D. V. Hoyt and J. A. Eddy, *Natl. Center Atmos. Res. Tech. Note NCAR/TN-194* (1982).
22. W. C. Livingston, L. Wallace, O. R. White, *Science* **240**, 1765 (1988).
23. J. R. Kuhn, K. G. Libbrechht, R. H. Dicke, *ibid.* **242**, 908 (1988).
24. Data used in this report were obtained from the National Space Science Data Center and the World Data Center, with the help of J. Closs and H. Coffey. B. Schlesinger provided the Mg index data. J. Hickey, R. Willson, D. Heath, and G. Rottman are responsible for solar irradiance measurements from the ERB, ACRIM, SBUV, and SME experiments, respectively. P. Foukal, H. Hudson, G. Rottman, and W. Livingston provided helpful comments on the manuscript.

21 October 1988; accepted 21 February 1989

Kestel: An Early Bronze Age Source of Tin Ore in the Taurus Mountains, Turkey

K. Aslihan Yener, Hadi Özbal, Ergun Kaptan, A. Necip Pehlivan, Martha Goodway

An ancient mine located at Kestel on the outskirts of Niğde, in the Taurus Mountains of south central Turkey, has been dated by radiocarbon and pottery type to the third millennium B.C. Archeological soundings in the mine located cassiterite (tin oxide) in the detritus of ancient mining activity. Cassiterite is also present in veins and, as placer deposits, in streams nearby. Since tin is used with copper in order to form bronze but is thinly distributed in the earth's crust, the presence of tin ore at Kestel offers a source for the much sought after tin of the Bronze Age. The discovery of an ancient mine containing cassiterite sheds light on this question, but also greatly complicates the accepted picture of regional economic patterns in the highland resource areas of Anatolia and of interregional metal exchange in the formative periods of urbanization and metal use in the eastern Mediterranean.

The Bronze Age began in southwestern Asia in the fourth millennium B.C. with the introduction of metal objects in which copper had been alloyed primarily with arsenic or tin. Metal assemblages excavated from major urban centers of ancient Anatolia, Syria, and Mesopotamia reveal the development of an alloy of copper with 5 to 10% tin (*1*). This development from arsenical copper to tin bronze occurred largely during the third millennium B.C. By the mid–second millen-

K. A. Yener and M. Goodway, The Conservation Analytical Laboratory, The Smithsonian Institution, Washington, DC 20560.
H. Özbal, Department of Chemistry, Boğaziçi University, PK2 Bebek, Istanbul, Turkey.
E. Kaptan, Museum of Natural History, Turkish Geological Research and Survey Directorate, Ankara, Turkey.
A. N. Pehlivan, Turkish Geological Research and Survey Directorate, Ankara, Turkey.